APPLIED ENERGY

Temperature control in 5th generation district heating and cooling networks: An MILP-based operation optimization

Marco Wirtz[a], Lisa Neumaier[a,b], Peter Remmen[a], Dirk Müller[a]

[a)] ***RWTH Aachen University***, *E.ON Energy Research Center, Institute for Energy Efficient Buildings and Indoor Climate, Mathieustr. 10, Aachen, Germany*
[b)] ***ETH Zurich***, *Energy & Process Systems Engineering, Tannenstrasse 3, 8092 Zurich, Switzerland*

Please cite journal article:
https://www.sciencedirect.com/science/article/pii/S0306261921001422

DOI: 10.1016/j.apenergy.2021.116608

Accepted manuscript

Temperature Control in 5th Generation District Heating and Cooling Networks: An MILP-based Operation Optimization

Marco Wirtz[a,*], Lisa Neumaier[a], Peter Remmen[a], Dirk Müller[a]

[a] *RWTH Aachen University, E.ON Energy Research Center, Institute for Energy Efficient Buildings and Indoor Climate, Mathieustr. 10, Aachen, Germany*

Abstract

In order to realize an energy efficient and emission-free heat and cold supply in urban areas, 5th Generation District Heating and Cooling (5GDHC) networks are a promising technology. In 5GDHC networks, the control of the network temperature is crucial since it affects the efficiency of connected heat pumps and chillers, the heat losses (or gains) of the network, as well as the integration of waste heat or free cooling. Due to the large number of opposing effects, the optimal control of network temperatures is a challenging task. In this paper, a mixed-integer linear program (MILP) is proposed for short-term optimization of the network temperature in 5GDHC systems. The model comprises an air-source heat pump, compression chiller and thermal storage in a central generation unit as well as heat pumps, chillers, electric boilers and thermal storages in buildings. Furthermore, the model considers the thermal inertia of the water mass in the network which functions as additional thermal storage. The optimization model is real-time capable

*Corresponding author

Email address: marco.wirtz@eonerc.rwth-aachen.de (Marco Wirtz)

and designed to be deployed in a model-predictive control. In a case study, the optimization approach leads to cost savings in two of three investigated months (by 10 % and 60 % respectively) compared to a reference operation strategy (free floating network temperature).
Keywords:
District heating, District cooling, 5GDHC, Operational optimization, MILP, Network temperature

1. Introduction

In Europe, 50 % of the final energy consumption results from the heating and cooling sector [1]. In order to achieve the goals of the Paris agreement, a fast and effective decarbonization of the heating and cooling sector is crucial. Especially in urban and industrial areas, district heating and cooling infrastructure is considered a key technology [2]. As of today, most of the European district heating networks are operated at high temperatures (above 70 °C) and supplied by burning fossil fuels [3]. The trend towards lower operating temperatures leads to lower heat losses and enables the integration of low-temperature heat sources, such as waste heat from data centers [4] or industry. The latest development stage in this trend are 5th generation district heating and cooling (5GDHC) networks which are operated at temperatures of 6 – 40 °C [5, 6]. At this temperature level, 5GDHC networks are able to supply buildings with both, heat and cold, making 5GDHC networks an ideal technology for the expected rise of cooling demands in the coming decades [7]. Buildings connected to the network are equipped with heat pumps which use the network as heat source in order to provide space

heating or domestic hot water preparation [8, 9, 10]. In recent literature, 5GDHC networks are also referred to as *bidirectional low temperature networks* [11, 12], *cold district heating* [13], *low-temperature district heating and cooling networks* [14, 15] or *balanced energy networks* [16].

The network temperature has a large impact on the performance of 5GDHC systems [17]. Firstly, the operating temperature affects heat losses (or gains): A low network temperature minimizes heat losses in winter; high network temperatures in summer lead to desired heat losses (surplus waste heat can be dissipated for free). Secondly, the network temperature strongly affects the coefficient of performance (COP) of heat pumps and chillers in buildings. For example, heat pumps in buildings are operated at a higher COP when the network temperature is high. Moreover, the temperatures of the network affect the operation of chillers in buildings: If the network temperature is low (e.g. $< 16\,^{\circ}\mathrm{C}$), chillers can be bypassed and direct cooling with the cold pipe of the network is enabled instead. Finally, the possibility of integrating heat or cold sources, e.g. ambient air, river or sea water, ground or sewage water, depends on the operating temperature of the network. The aforementioned effects are partially conflicting and, as a result, the optimization of the network temperature of a 5GDHC system is a challenging task [18]. Boesten et al. [3] indicate that existing energy hub optimization concepts need to be enhanced, especially regarding modeling floating temperature levels, and proposes to investigate the optimization of the network temperatures.

One approach to optimize the operation of 5GDHC network is presented by Prasanna et al. [19]. They formulate an MILP for an operation optimiza-

tion of all energy conversion and storage units in the system. However, the network temperatures are not explicitly modeled or optimized and constant average COPs for heat pumps in buildings are assumed. Buffa et al. [20] present a control approach for substations in 5GDHC networks using artificial neural networks. While this approach improves the operation of substations in buildings, it does not optimize network temperatures. A review of similar control applications using artificial neural networks is provided in [21].

Two approaches have been presented in literature that aim at optimizing network temperatures for 5GDHC networks: Bünning et al. [11] propose a mathematical relation between the network temperature and the heating and cooling demands. However, this temperature control strategy is a heuristic approach which does not account for heat losses of the network, the COP of connected heat pumps and chillers or temperature thresholds of direct cooling. The authors of [11] find that the effect of the proposed temperature control strategy is small and assuming a constant temperature only leads to a small performance decline.

Gabrielli et al. [22] present a mixed-integer non-linear program for the operation optimization of the 5GDHC network at ETH Zurich using bilinear products of mass flow rate and fluid temperature ($\dot{m}T$). To cope with the high computational complexity, they derive an MILP by linearizing the efficiency curves of the heat pumps and assuming a fixed profile for the mass flow rate. The low temperature variations in the investigated 5GDHC network allow replacing the highly non-linear relation between heat output, electric power and inlet temperature at the evaporator of the heat pump with a bivariate linear approximation. However, for 5GDHC networks operating with larger

temperature fluctuations, the linear approximation leads to significant errors and is therefore not applicable.

A simple yet robust heuristic temperature control approach, called *free-floating temperature control*, is described by Blacha et al. [23] and Pass et al. [24]: The network fluid is heated or cooled by an external supply (e.g. energy hub) only if the network temperature is about to drop below a lower or about to exceed an upper temperature limit. For example, if due to a high heat demand in winter, the temperature of the warm pipe reaches the lower limit (e.g. 10 °C), the energy hub starts to operate and heats the network in order to prevent a further drop of the network temperature. This temperature control strategy is robust and straightforward to implement but does not achieve an optimal system performance since it does not account for network heat losses or temperature-dependent efficiencies of heat pumps and chillers.

While for 5GDHC networks, no control approach for optimizing the system operation and network temperatures has been presented, the optimization of supply temperatures in conventional district heating networks is common practice and has been extensively investigated in literature. In the following, a brief overview is presented:

Vandermeulen et al. [25] provide a comprehensive review of state-of-the-art control strategies for conventional district heating systems and how flexibility potentials can be exploited by heat storages as well as the thermal inertia of buildings and the water mass in the network. However, the review is limited to conventional district heating and no control stategies applicable for 5GDHC systems are presented.

Another comprehensive review of different models suitable for short-term operational optimization is presented by Bøhm et al. [26] who also focus on conventional district heating. A non-linear supply temperature optimization approach is presented and applied to a use case in Germany.

Benonysson et al. [27] formulate a mathematical model for conventional district heating networks based on the so-called *node method*. The model describes all mass flows and temperatures in all pipe segments. However, pressure states and hydraulic relations are not included in the model which hinders the calculation of mass flows in a bidirectional 5GDHC network with undefined flow directions.

Leśko et al. [28] compare two operational optimization approaches, one topology-based approach and one method based on delay times of the water flow in the network. In the presented cost optimization, the benefit of using the thermal inertia of the network is investigated.

Grosswindhager et al. [29] present a fuzzy direct matrix control (fuzzy DMC) for supply temperatures in district heating networks. They show that a fuzzy DMC is a suitable approach to handle the inherent non-linearity of district heating responses.

Merkert et al. [30] propose an MILP for short-term optimization of the supply temperature of a district heating network. The optimization determines the point of time when the network is heated up and the corresponding temperature increase. According to the model, the temperature propagation wave reaches the buildings after a temporal network delay which is known a-priori.

Gu et al. [31] propose a mixed-integer non-linear program (MINLP) for

the control of a district heating network. Assuming constant mass flows in all pipe segments, the network temperature of every segment is optimized. The flexibility potential of the thermal inertia of the network and buildings is used to minimize operational costs and curtailment of renewable energy sources.

In summary, the aforementioned operational optimization approaches have been developed for conventional district heating systems in which the flow direction in each pipe segment is known. In these conventional, unidirectional networks the supply temperature is used as control variable and optimized with forecasts of the heat demand or ambient air temperature. However, these approaches cannot be adapted to networks with undirected mass flows which occur in bidirectional 5GDHC networks. This paper aims at closing this gap by presenting an operation optimization model, in form of an MILP, which optimizes the operation of all energy conversion and storage units as well as the network temperatures of a 5GDHC system. The contributions of this paper are described in the following Section 1.1 in detail.

1.1. Contributions

In this paper, a novel operation optimization model for 5GDHC networks is presented. It is designed to be used in a model predictive control (MPC) as depicted in Fig. 1. The model optimizes the operation of all generation and storage units of the system as well as the network temperature profile. The optimization considers the non-linear relation between network temperature and coefficient of performance (COP) of the connected heat pumps and chillers as well as heat losses and gains of the network. In order to cope with the non-linear relation between network temperature and COP, a

novel MILP formulation using binary variables is presented. Unlike previous studies, the model formulation considers the thermal inertia of the following three components: Central storage unit (accumulator tank), decentral thermal storages in every building and the water mass in the network. Within a case study, the following research questions are investigated:

- Which physical effect has the largest impact on the optimal network temperature?
- To what extent do a central storage unit and the thermal inertia of the network support the balancing process of heating and cooling demands in 5GHDC networks?
- Which cost savings are achieved by a temperature optimization model compared to conventional operation strategies (free floating network temperature and constant network temperature)?

1.2. Paper organization

The structure of this paper is as follows: In Section 2, the methodology is introduced. At first, the structure and operating principle of the 5GDHC system are described. Then, the MILP is presented in detail including all model assumptions. The use case is introduced in Section 3. The optimal temperature control strategy is analyzed for three representative months in Section 4. Section 5 provides final conclusions.

2. Methodology

In the following Section 2.1, the concept of 5GDHC networks is described and the system structure investigated in this study is explained in more

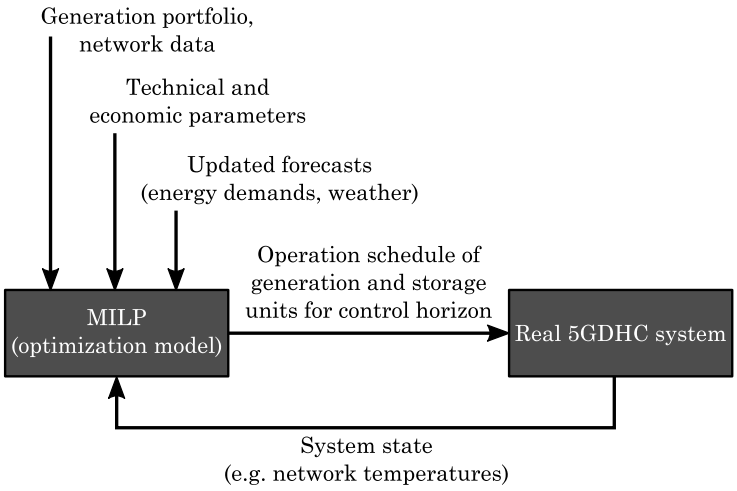

Figure 1: Integration of optimization model in system control strategy (model predictive control).

detail. The MILP is presented in Section 2.2.

2.1. Working principle of 5GDHC networks

5GDHC networks consist of a warm and a cold pipe which are both operated at temperatures close to the surrounding (6 – 40 °C). In each building, a heat pump raises the temperature to the required supply temperature of the building's heating system. Heat pumps use water from the warm network pipe as heat source in the evaporator. After passing the heat pump, the cooled down water is discharged to the cold pipe. Buildings with a cooling demand use water from the cold network pipe as heat sink and discharge the warmed up water to the warm pipe. Depending on the temperature requirements of the cooling circuit in the building, chillers or heat exchangers are installed in buildings. With heat exchangers in the building, heat is directly transferred from the building's cooling system to thermal network

(direct cooling). Through the bidirectional network, buildings with cooling demands supply buildings with heating demands with low temperature waste heat. In times with an excess of waste heat (or cold), the network is cooled (or heated) by a central generation unit, e.g. an energy hub (EH). The central generation unit ensures that the temperatures of the warm and cold pipe stay within a defined temperature range. In order to support balancing of heating and cooling demands between buildings, a thermal storage (accumulator tank, ACC) can be connected to the network [5, 24]. An ACC is a large water tank which is hydraulically connected at the top with the warm network pipe and on the bottom with the cold network pipe. For significant temperature differences between the warm and cold pipe (approx. $> 4\,\mathrm{K}$), a temperature stratification in the tank is observed. As a result, warm water is located at the top of the tank and cold water at the bottom. The ACC functions as passive element to balance residual heating and cooling demands of the network: When the buildings induce a net mass flow from the warm pipe to the cold pipe (e.g. when on a cold day a large amount of heat pumps in buildings are operated), mass conservation causes cold water to enter the tank at the bottom and warm water from the top of the tank flows into the warm pipe. As a result, the volume of the cold water at the bottom of the tank increases and the volume of the warm water decreases. In this case, as long as the water in the ACC is not fully at cold pipe temperature, the ACC can balance the residual building demands and the EH does not need to be operated. The ACC operation in a 5GDHC system is further described in [5].

Fig. 2 shows the energy system structure investigated in this study with an

EH, ACC and a representative building energy system. The EH comprises an air source heat pump and compression chiller for balancing residual demands of the 5GDHC network. For electricity generation photovoltaic modules are considered. Excess power can be fed into the electricity grid. On the right hand side of Fig. 2, the building energy system for one exemplary building is depicted. For covering cooling demands, a compression chiller and a heat exchanger for direct cooling with the cold pipe of the 5GHDC network is considered. The condenser of the chiller is hydraulically connected with the 5GDHC network and discharges warmed water to the warm network pipe. If the network temperature is lower than the supply temperature of the cooling circuit in the building, the building's cooling demand is covered with the heat exchanger (direct cooling). For covering the buildings' heating demand, a heat pump connected to the 5GDHC network, an electric boiler as well as a heat storage are considered.

In this 5GDHC system configuration, the ACC, the network's water mass and the decentral storages increase the operation flexibility: The thermal inertia of the ACC and the network can be used as thermal storage and can support the balancing of residual heating and cooling demands over time. In addition, the thermal storages in buildings increase the operational flexibility of the building energy system.

2.2. Mixed-integer linear program

This section presents the operation optimization model which is adapted from a design optimization model presented in [32]. Decision variables are written in italics while model parameters are written in non-italics. All continuous decision variables are greater or equal to zero, unless otherwise stated.

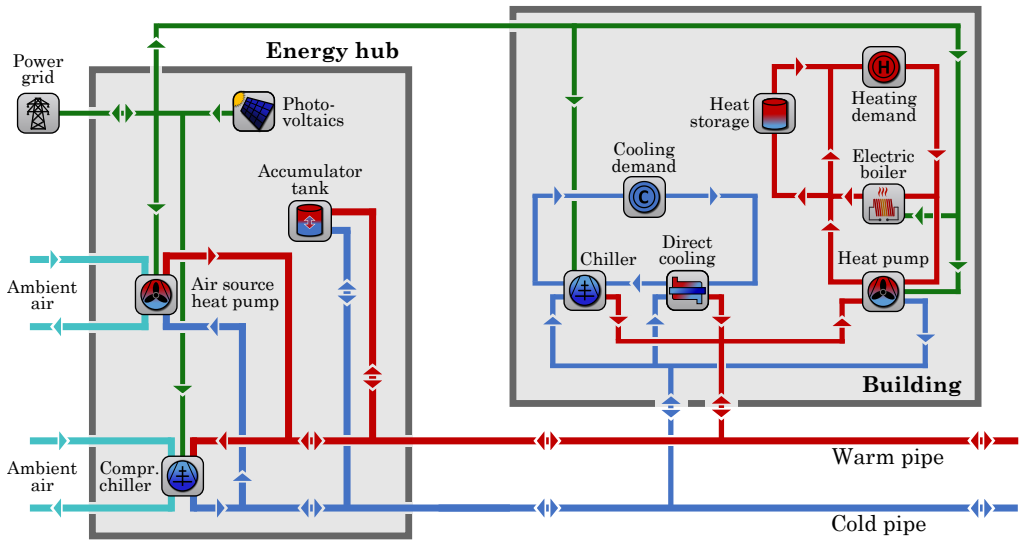

Figure 2: Structure of the investigated 5GDHC system with energy hub, accumulator tank and building energy system.

2.2.1. Objective function

The objective function are the operational costs C_{op} of the 5GDHC system:

$$C_{\mathrm{op}} = \mathrm{p}_{\mathrm{el,sup}} \sum_{t \in \mathcal{T}} P_{\mathrm{el,grid},t}\, \Delta \mathrm{t}_t - \mathrm{p}_{\mathrm{el,feed\text{-}in}} \sum_{t \in \mathcal{T}} P_{\mathrm{el,feed\text{-}in},t}\, \Delta \mathrm{t}_t \tag{1}$$

Here, $P_{\mathrm{el,grid},t}$ denotes the power imported from an external electricity grid and $P_{\mathrm{el,feed\text{-}in},t}$ excess power that is fed in. $\mathrm{p}_{\mathrm{el,sup}}$ and $\mathrm{p}_{\mathrm{el,feed\text{-}in}}$ denote the electricity supply price and feed-in revenue, respectively. $\Delta \mathrm{t}_t$ is the duration of the respective time step t.

2.2.2. Energy balances

The optimization model comprises four sets of thermal energy balances: The first set describes the energy balances for every building b and every

time step t:

$$\begin{aligned}\dot{Q}_{\mathrm{res,BES},b,t} = (\dot{Q}_{\mathrm{HP},b,t} - P_{\mathrm{HP},b,t}) \\ - (\dot{Q}_{\mathrm{CC},b,t} + P_{\mathrm{CC},b,t}) - \dot{Q}_{\mathrm{DRC},b,t} \quad \forall\, b \in \mathrm{B},\ t \in \mathcal{T}\end{aligned} \tag{2}$$

$\dot{Q}_{\mathrm{res,BES},b,t}$ denotes the residual heating or cooling demand of a building. A positive residual demand corresponds to a residual heating demand while a negative residual demand corresponds to a residual cooling demand. The term $(\dot{Q}_{\mathrm{HP},b,t} - P_{\mathrm{HP},b,t})$ is the heat to the evaporator of the heat pump and the term $(\dot{Q}_{\mathrm{CC},b,t} + P_{\mathrm{CC},b,t})$ the waste heat of the chiller.

The second set of energy balances describe heat flows to and from the network fluid:

$$\dot{Q}_{\mathrm{res,netw},t} = \sum_{b \in \mathrm{B}} (\dot{Q}_{\mathrm{res,BES},b,t}) + \dot{Q}_{\mathrm{loss,wp},t} - \dot{Q}_{\mathrm{loss,cp},t} + \dot{Q}_{\mathrm{netw},t} \quad \forall\, t \in \mathcal{T} \tag{3}$$

$\dot{Q}_{\mathrm{res,netw},t}$ denote the residual network demand. The heat losses of the warm and cold pipe ($\dot{Q}_{\mathrm{loss,wp},t}$ and $\dot{Q}_{\mathrm{loss,cp},t}$) are decision variables since they depend on the network temperature, see Section 2.2.4. $\dot{Q}_{\mathrm{netw},t}$ describes the thermal power to raise or lower the network temperature.

The third set of energy balances describe the charging and discharging of the ACC:

$$\dot{Q}_{\mathrm{res,EH},t} = \dot{Q}_{\mathrm{res,netw},t} + \dot{Q}_{\mathrm{ACC},t} \quad \forall\, t \in \mathcal{T} \tag{4}$$

The variable $\dot{Q}_{\mathrm{ACC},t}$ denotes the charging or discharging power of the ACC: $\dot{Q}_{\mathrm{ACC},t} > 0$ means water from the warm pipe of the network enters the ACC and cold water from the bottom of the tank flows into the cold pipe. $\dot{Q}_{\mathrm{ACC},t} < 0$ describes the reverse process and, as a result, a decrease of the

mean ACC temperature. $\dot{Q}_{\mathrm{res,EH},t}$ is the thermal power provided by the EH to the network. $\dot{Q}_{\mathrm{res,EH},t} > 0$ means the EH heats the network; $\dot{Q}_{\mathrm{res,EH},t} < 0$ means the EH cools the network.

The last set of energy balances describe the heat and cold generation by the air source heat pump (ASHP) and compression chiller (CC) in the EH:

$$\dot{Q}_{\mathrm{res,EH},t} = \dot{Q}_{\mathrm{h,ASHP},t} - \dot{Q}_{\mathrm{c,CC},t} \quad \forall\, t \in \mathcal{T} \tag{5}$$

The coefficients of performance of the ASHP and chiller are calculated with the ambient air temperature for every network temperature prior to the optimization.

Additionally, the optimization model comprises electric energy balances. The electricity demand of the building energy system $P_{\mathrm{BES},b,t}$ is

$$P_{\mathrm{BES},b,t} = P_{\mathrm{EB},b,t} + P_{\mathrm{HP},b,t} + P_{\mathrm{CC},b,t} \quad \forall\, b \in \mathrm{B},\ t \in \mathcal{T}, \tag{6}$$

where $P_{\mathrm{EB},b,t}$, $P_{\mathrm{HP},b,t}$ and $P_{\mathrm{CC},b,t}$ denote the electric power of the electric boiler, heat pump, and compression chiller, respectively.

The total electricity demand of the system is the sum of all building electricity demands ($P_{\mathrm{BES},b,t}$), the electricity demands of the EH ($P_{\mathrm{ASHP},t}$ and $P_{\mathrm{CC},t}$), and the excess power fed into the electricity grid ($P_{\mathrm{el,feed\text{-}in},t}$). The total electricity demand is covered by PV generation ($P_{\mathrm{PV},t}$) and the power imported from the grid ($P_{\mathrm{el,grid},t}$):

$$P_{\mathrm{el,grid},t} + P_{\mathrm{PV},t} = \sum_{b \in \mathrm{B}} (P_{\mathrm{BES},b,t}) + P_{\mathrm{ASHP},t} + P_{\mathrm{CC},t} + P_{\mathrm{el,feed\text{-}in},t} \quad \forall\, t \in \mathcal{T} \tag{7}$$

2.2.3. Network temperature intervals

In order to describe the network fluid temperature, three temperature variables are introduced for every time step t: The temperature of the warm

pipe ($T_{\mathrm{netw,w},t}$), cold pipe ($T_{\mathrm{netw,c},t}$) and a mean network temperature ($\overline{T}_{\mathrm{netw},t}$):

$$T_{\mathrm{netw,w},t} = \overline{T}_{\mathrm{netw},t} + \frac{\Delta \mathrm{T}_{\mathrm{netw}}}{2}, \tag{8}$$

$$T_{\mathrm{netw,c},t} = \overline{T}_{\mathrm{netw},t} - \frac{\Delta \mathrm{T}_{\mathrm{netw}}}{2} \quad \forall\, t \in \mathcal{T} \tag{9}$$

The temperature difference between the warm and cold pipe is assumed constant ($\Delta \mathrm{T}_{\mathrm{netw}} = 8\,\mathrm{K}$, [8]). Network temperatures are limited to a predefined range [$\mathrm{T}^{\mathrm{min}}_{\mathrm{netw,c}}$, $\mathrm{T}^{\mathrm{max}}_{\mathrm{netw,w}}$] with $\mathrm{T}^{\mathrm{min}}_{\mathrm{netw,c}} = 6\,^{\circ}\mathrm{C}$ and $\mathrm{T}^{\mathrm{max}}_{\mathrm{netw,w}} = 40\,^{\circ}\mathrm{C}$ [8]. This range is subdivided into $\mathrm{n}_{\mathrm{int}}$ discrete temperature intervals [$\mathrm{T}_{\mathrm{low},k}$, $\mathrm{T}_{\mathrm{up},k}$] $\forall\, k \in \{0, ..., \mathrm{n}_{\mathrm{int}} - 1\}$ with constant interval width $\Delta \mathrm{T}_{\mathrm{int}}$:

$$\mathrm{T}_{\mathrm{up},k} = \mathrm{T}^{\mathrm{min}}_{\mathrm{netw,c}} + \frac{\Delta \mathrm{T}_{\mathrm{netw}}}{2} + (k+1)\Delta \mathrm{T}_{\mathrm{int}} \tag{10}$$

$$\mathrm{T}_{\mathrm{low},k} = \mathrm{T}^{\mathrm{min}}_{\mathrm{netw,c}} + \frac{\Delta \mathrm{T}_{\mathrm{netw}}}{2} + k\Delta \mathrm{T}_{\mathrm{int}} \tag{11}$$

If the mean network temperature is in the interval [$\mathrm{T}_{\mathrm{low},k}$, $\mathrm{T}_{\mathrm{up},k}$], the temperature interval is active and the binary variable $\theta_{k,t}$ equals 1. The constraint

$$\sum_{k=0}^{\mathrm{n}_{\mathrm{int}}-1} \theta_{k,t} = 1 \quad \forall\, t \in \mathcal{T} \tag{12}$$

ensures that exactly 1 interval is active at time step t. A set of disjunctive inequalities force $\theta_{k,t}$ to be 1 only if the mean network temperature is in the corresponding interval [33]. The disjunctive inequalities corresponding to the temperature intervals are implemented using the convex-hull reformulation by Jeroslow & Lowe [34]. Consequently, the variable $T^{\theta}_{k,t}$ is introduced and forced to take the value of the mean network temperature if the interval k is active:

$$T^{\theta}_{k,t} \geq \theta_{k,t}\, \mathrm{T}_{\mathrm{low},k}, \tag{13}$$

$$T^{\theta}_{k,t} \leq \theta_{k,t}\, \mathrm{T}_{\mathrm{up},k} \quad \forall\, k \in \{0, ..., \mathrm{n}_{\mathrm{int}} - 1\},\ \forall\, t \in \mathcal{T} \tag{14}$$

The mean network temperature is then the sum of all variables $\mathrm{T}_{k,t}^{\theta}$:

$$\overline{T}_{\mathrm{netw},t} = \sum_{k=0}^{\mathrm{n_{int}}-1} T_{k,t}^{\theta} \quad \forall\, t \in \mathcal{T} \tag{15}$$

2.2.4. Heat losses

Heat losses of the network depend linearly on the temperature difference between network fluid and the surrounding soil: The heat losses of the warm pipe $\dot{Q}_{\mathrm{loss,wp},t}$ are

$$\dot{Q}_{\mathrm{loss,wp},t} = (\mathrm{kA})_{\mathrm{netw}} (T_{\mathrm{netw,w},t} - \mathrm{T}_{\mathrm{soil},t}) \quad \forall\, t \in \mathcal{T} \tag{16}$$

and of the cold pipe

$$\dot{Q}_{\mathrm{loss,cp},t} = (\mathrm{kA})_{\mathrm{netw}} (\mathrm{T}_{\mathrm{soil},t} - T_{\mathrm{netw,c},t}) \quad \forall\, t \in \mathcal{T} \tag{17}$$

The heat loss coefficient $(\mathrm{kA})_{\mathrm{netw}}$ and the soil temperature $\mathrm{T}_{\mathrm{soil},t}$ are based on the case study presented in [32].

2.2.5. Coefficient of performance and direct cooling

The COPs of heat pumps and chillers are calculated for each time step t and each network temperature interval k prior to the optimization (calculation according to [32] and [35]). For a heat pump or a chiller, the energy balance is

$$\dot{Q}_t = \sum_{k=0}^{\mathrm{n_{int}}-1} \Big[\mathrm{COP}_{k,t}\, \theta_{k,t} \Big] P_t \tag{18}$$

where $\dot{Q}_t$ denotes the device's heating or cooling power and P_t the electric power consumption. The product is linearized by introducing an auxiliary

variable $P^{\theta}_{k,t}$ [33]. If the interval k is active, $P^{\theta}_{k,t}$ equals the electric power consumed by the component P_t, otherwise it is 0. Thus, Eq. (18) is reformulated as

$$\dot{Q}_t = \sum_{k=0}^{\mathrm{n_{int}}-1} \left[\mathrm{COP}_{k,t}\, P^{\theta}_{k,t} \right] \quad \forall\ t\ \in\ \mathcal{T} \tag{19}$$

The auxiliary variable $P^{\theta}_{k,t}$ is constrained by

$$P^{\theta}_{k,t} \leq \theta_{k,t}\, \mathrm{M_P}, \tag{20}$$

$$P^{\theta}_{k,t} \leq P_t, \tag{21}$$

$$\begin{aligned} P^{\theta}_{k,t} &\geq P_t - (1-\theta_{k,t})\, \mathrm{M_P} \\ &\forall\ k\ \in\ \{0, ..., \mathrm{n_{int}}-1\},\ \forall\ t\ \in\ \mathcal{T}. \end{aligned} \tag{22}$$

2.2.6. Direct cooling

The network temperature determines if direct cooling (DRC) in buildings is possible. Direct cooling is realized with a heat exchanger which uses the cold network pipe to cool the building's cooling circuit without electric power. The binary variable $y_{\mathrm{DRC},b,t}$ is introduced to indicate if the network temperature is low enough for direct cooling to take place. Depending on the temperature difference between warm and cold pipe ($\Delta \mathrm{T_{netw}}$) and the temperature difference of supply and return temperature of the building's cooling circuit ($\mathrm{T_{c,return},b,t} - \mathrm{T_{c,supply},b,t}$), the pinch is either on the cold or on the warm side of the heat exchanger. Therefore, if $\mathrm{T_{c,return},b,t} - \mathrm{T_{c,supply},b,t} \geq \Delta \mathrm{T_{netw}}$ holds, the constraints

$$\begin{aligned} T_{\mathrm{netw,c},t} + \Delta \mathrm{T_{min}} - \mathrm{T_{c,supply},b,t} \leq & (1 - y_{\mathrm{DRC},b,t}) \mathrm{M_{DRC},b} \\ & \forall\ t\ \in\ \mathcal{T},\ b\ \in\ \mathrm{B} \end{aligned} \tag{23}$$

are added to the model, otherwise the constraints

$$T_{\mathrm{netw,h},t} + \Delta \mathrm{T}_{\min} - \mathrm{T}_{\mathrm{c,return},b,t} \leq (1 - y_{\mathrm{DRC},b,t}) \mathrm{M}_{\mathrm{DRC},b} \quad \forall\, t \in \mathcal{T},\ b \in \mathrm{B} \tag{24}$$

are used. Here, $\Delta \mathrm{T}_{\min}$ is the minimum temperature difference across the heat exchanger and $\mathrm{M}_{\mathrm{DRC},b}$ is a big-M coefficient [36]. Eqs. (23) and (24) force the binary variable $y_{\mathrm{DRC},b,t}$ to 1 if direct cooling can be used. Eq. (25) limits the cooling power to the rated power of the heat exchanger (for $y_{\mathrm{DRC},b,t} = 1$) and for $y_{\mathrm{DRC},b,t} = 0$ the cooling power is 0:

$$\dot{Q}_{\mathrm{c,DRC},b,t} \leq y_{\mathrm{DRC},b,t}\, \mathrm{Q}^{\mathrm{nom}}_{\mathrm{c,DRC},b} \quad \forall\, t \in \mathcal{T} \tag{25}$$

2.2.7. Storage and network temperature

Excess heat from buildings or heat generated in the EH can be used to increase the temperature of the network. The mean network temperature of two consecutive time steps ($\overline{T}_{\mathrm{netw},t}$ and $\overline{T}_{\mathrm{netw},t-1}$) are connected by

$$\overline{T}_{\mathrm{netw},t} = \overline{T}_{\mathrm{netw},t-1} + \Delta T_t \quad \forall\, t \in \mathcal{T} :\ t \neq t_0 \tag{26}$$

in which ΔT_t denotes the temperature increase. The ACC is thermally and hydraulically coupled with the network. As modeled in [5], the ACC is operated as passive balancing unit in the following way: For balancing residual network demands of the buildings, in the first stage, the ACC is used to provide heating or cooling power. In a second stage, when the ACC is fully charged (water of the ACC is at temperature of the warm pipe) or fully discharged (water is at temperature of cold pipe), the temperature of the network and the ACC can be raised or lowered. The thermal power for increasing or lowering the temperature of the water mass in the network and

the ACC is

$$\dot{Q}_{\mathrm{netw},t} = \rho_{\mathrm{W}} \left(\mathrm{V_{netw}} + \mathrm{V_{ACC}}\right) \mathrm{c_W} \, \Delta T_t \, \frac{1}{\Delta \mathrm{t}_t} \quad \forall \, t \in \mathcal{T} \tag{27}$$

$\dot{Q}_{\mathrm{netw},t}$ can take positive and negative values and is linked with the energy balance in Eq. (3). ρ_{W} and $\mathrm{c_W}$ denote the density and heat capacity of water. The water volume in the network ($\mathrm{V_{netw}}$) and in the ACC ($\mathrm{V_{ACC}}$) are model parameters. For modeling the ACC's operation strategy, two binary variables are introduced: $y_{\mathrm{inc},t}$ can be become 1 if the mean network temperature is increased, while $y_{\mathrm{dec},t}$ can become 1 if the mean network temperature is decreased. The network temperature change ΔT_t is linked with the binary decision variables by

$$\Delta T_t \leq y_{\mathrm{inc},t} \, \mathrm{M_T}, \tag{28}$$

$$\Delta T_t \geq -y_{\mathrm{dec},t} \, \mathrm{M_T} \quad \forall \, t \in \mathcal{T} \tag{29}$$

with a sufficiently large big-M coefficient ($\mathrm{M_T} = \mathrm{T^{max}_{netw,w}} - \mathrm{T^{min}_{netw,c}}$) [36]. The binary variables are linked with the ACC's state of charge by Eqs. (30) and (31). $y_{\mathrm{inc},t}$ can only take the value 1 if the ACC's storage level is at maximum in t and in $t-1$:

$$2 \, \mathrm{S^{cap}_{ACC}} \, y_{\mathrm{inc},t} \leq S_{\mathrm{ACC},t} + S_{\mathrm{ACC},t-1} \quad \forall \, t \in \mathcal{T} : \; t \neq t_0 \tag{30}$$

Accordingly, $y_{\mathrm{dec},t}$ can only take the value 1 if the ACC is fully discharged in t and in $t-1$:

$$2 \, \mathrm{S^{cap}_{ACC}} \, (1 - y_{\mathrm{dec},t}) \geq S_{\mathrm{ACC},t} + S_{\mathrm{ACC},t-1} \quad \forall \, t \in \mathcal{T} : \; t \neq t_0 \tag{31}$$

2.2.8. Free-floating network temperature operation (reference case)

In order to evaluate the performance of the optimized temperature operation, a free-floating temperature operation (as described in [23] and [24]) is

investigated as a reference. In the free-floating temperature operation, the network temperature is only driven by residual heating and cooling demands. Only, if the network temperature reaches an upper or lower limit ($T^{min}_{netw,c}$ = 6 °C, $T^{max}_{netw,w}$ = 40 °C), the network is heated or cooled which is ensured by additional constraints in the model. In the free-floating temperature operation, the same components are used in the EH and building energy systems and, in particular, direct cooling is possible. A performance comparison between the free-floating temperature operation and the optimized temperature operation is presented in Section 4.4.

2.2.9. Model limitations

Relevant model limitations result from the spatial resolution of the model: The water in the warm and cold pipe of the network are assumed as ideally mixed water volumes (as described by Leśko et al. [28]) and no hydraulic limitations of the network are considered. Thus, residual building demands can be balanced instantaneously within the duration of a time step and independently of their location in the district. This assumption is justified for small networks and large time steps, i.e. the network fluid can flow from one building to all other buildings within one time step.

In addition, a constant temperature difference between warm and cold pipe is assumed like in the model by Prasanna et al. [19]. For a system with temperature controlled heat pumps and chillers, this assumption appears to be valid. Even if the temperature difference in the real system is not exactly constant, this primarily affects the hydraulic states of the network, i.e. mass flows and pumping power. Only in the second place, it leads to a decline of accuracy of the COP and heat loss estimation of the model.

Moreover, a perfect temperature stratification of the fluid in the ACC is assumed and heat losses are neglected. An operation strategy of the ACC is prescribed in the model (in accordance to [5]): It is ensured that the ACC is fully charged (or discharged) before the network temperature can rise (or drop). In addition, all technologies are modeled with a low level of detail, e.g. part-load limitations, part-load efficiencies and minimum down times are not considered. Lastly, the optimization aims at minimizing the total operational costs of the entire energy supply system. However, in practice, the operator of the energy hub and thermal network may differ from the operators of the building energy systems. In this case, from the individual operator's perspective different network temperatures would be considered cost-optimal: In winter, for example, the buildings' operator would prefer high network temperatures (to achieve high heat pump COPs) while the network operator prefers low network temperatures.

3. Use case

In this section, the case study and the investigated scenarios are presented. Section 3.1 provides a brief description of the case study. The installed generation and storage capacities in the assumed 5GDHC system are presented in Section 3.2. Section 3.3 introduces the investigated scenarios.

3.1. Use case description

The use case is a German research campus for which 17 buildings are considered including laboratories, office buildings, two data centers and a canteen. For the heating systems of the buildings, a required supply temperature of 60 °C is assumed and for cooling 16 °C. A detailed description of

the use case is presented in [32]. Currently, no 5GDHC network exists on the research campus but the heating and cooling demands appear to be a realistic use case for a 5GDHC network and therefore the district is used in this study. The total heating demand of all buildings is 6.36 GWh with a peak heating demand of 2.01 MW and the total cooling demand is 10.04 GWh with a peak cooling demand of 2.42 MW. Fig. 3 shows the annual time series of the cumulated heating and cooling demands. In the case study, the electricity supply price is assumed 0.1523 EUR/kWh [37] and the feed-in revenue 0.085 EUR/kWh [38]. Energy conversion efficiencies as well as the weather data used in the case study are based on [32].

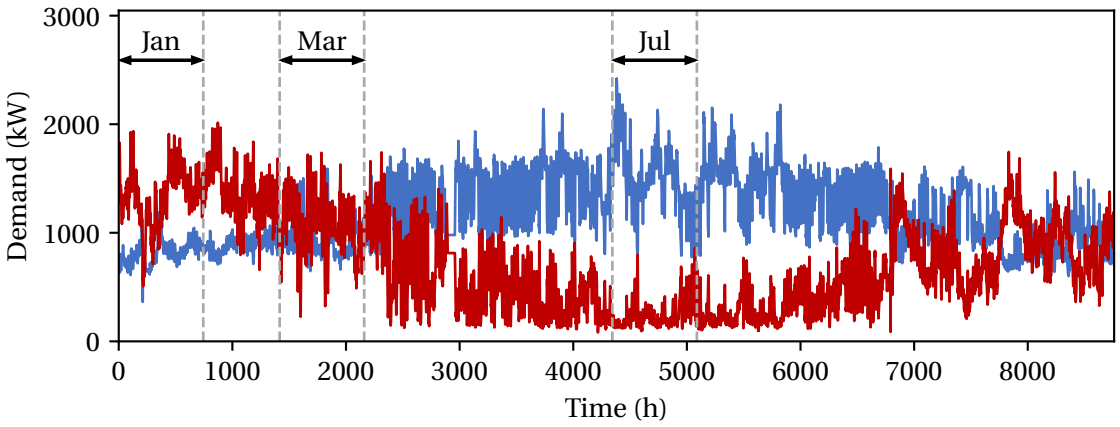

Figure 3: Cumulated heating (red) and cooling demands (blue) of all 17 buildings. January, March and July are investigated in the case study. Illustration based on [32].

3.2. Energy system

Since on the research campus no 5GDHC network exists, for all buildings and the EH, the installed capacities of all generation and storage technologies

have to be assumed. The capacities are calculated with a design optimization approach based on a model presented in [32]. In the EH, an ASHP and a compression chiller are installed with a rated heating and cooling capacity of 1.13 MW_{th} and 2.51 MW_{th}, respectively. The installed peak power of PV modules is assumed 1.02 MW_p. The ACC has a tank volume of 95.4 m^3 which equals a storage capacity of 0.89 MWh. In the building energy systems, compression chillers and heat exchangers for direct cooling are installed with a thermal capacity of 2.88 MW_{th} and 1.98 MW_{th}, respectively. For heating, the building energy systems comprise heat pumps with a cumulated thermal power of 1.64 MW_{th}, electric boilers with 0.77 MW_{th} and thermal energy storages with a cumulated capacity of 2.02 MWh.

For the 5GDHC network in this case study, the assumed topology and design has been adopted from [32]: The network length is 1.3 km, the minimum pipe diameter 55 mm and the maximum diameter 141 mm. The water volume in the pipes is 10.3 m^3 and the $(kA)_{netw}$-value 3.7 kW/K. In the case study, a maximal network temperature of $T^{max}_{netw,w}$=40 °C and a minimum network temperature of $T^{min}_{netw,c}$=6 °C are considered. The difference between the warm and cold pipe is ΔT_{netw}=8 K. The temperature range between the maximum mean network temperature (36 °C) and the minimum mean network temperature (10 °C) is subdivided into 4 intervals.

3.3. Investigated scenarios

Two energy system configurations (OPT-DRC and OPT) are investigated: In the configuration OPT-DRC, compression chillers and direct cooling are enabled for the cooling system in buildings. In the scenario OPT, only compression chillers are enabled, while direct cooling is not available.

The investigation of two scenarios is necessary since the optimal network temperature substantially depends on whether direct cooling in buildings is possible or not.

In this work, three representative months are selected based on their heating and cooling demand profiles. The heating and cooling demands, the demand ratio and the demand overlap coefficient [39] (definitions provided in Appendix A) of the three months are shown in Table 1. January is chosen as the month with the highest demand ratio indicating that heating demands dominate. March is chosen as a month with alternating demands. The demand ratio is close to 0 and a large heating and cooling demand overlap is observed. In July, the cooling demands dominate and the peak cooling demand is observed. The cumulated demand profiles are depicted in Fig. 3.

Table 1: Total monthly heating and cooling demands, demand ratio and demand overlap coefficient. For the case study, a month with dominating heating demand (January), a month with balanced heating and cooling demands (March) and a month with dominating cooling demands (July) are investigated.

Month	Heating demand	Cooling demand	Demand ratio	Demand overlap coefficient [39]
January	991.0 MWh	603.5 MWh	0.24	0.75
March	789.2 MWh	691.3 MWh	0.07	0.84
July	187.3 MWh	1119.8 MWh	−0.71	0.29

The optimization is repeatedly executed in a rolling horizon framework. In this study, a control horizon of 6 h (6 time steps in hourly resolution) and an overlap horizon (foresight) of 36 h with 6-hourly resolution is chosen. The temporal aggregation is based on a downsampling approach described

by Cao et al. [40].

4. Results

In this section, the results of the system configurations OPT-DRC and OPT (optimized temperature with and without direct cooling) are presented. The mean computing time for optimizing one control interval (6 hours) was in all scenarios less than 5 minutes and the computing time for one month was less than 10 hours. Therefore, the model is real-time capable and can be employed in a model predictive control.

4.1. Operational costs

The operational costs only consist of electricity costs. The monthly costs are listed for January, March and July in Table 2. The highest operational costs are observed in January due to two reasons: Firstly, the heating demands dominate and substantially outbalance the low cooling demands. Covering heating demands is in general more cost-intensive than covering cooling demands as the heat pump COP is lower than the chiller COP. Secondly, less PV power is generated in January due to the lower solar radiation. This increases the electricity imported from the electricity grid and reduces feed-in revenues. The system configuration with direct cooling in buildings (OPT) shows lower costs for all three months. However, the cost difference strongly depends on the month: In January, the OPT-DRC configuration results in cost savings of only 9.8 %. In July, the cost savings are substantially higher (57.7 %). This indicates that direct cooling is advantageous during months with dominating cooling demands. This effect will be explained in more detail by analyzing the network temperature profiles in Section 4.2.

Table 2: Operational costs for the investigated months.

Month	OPT-DRC (EUR)	OPT (EUR)
January	36,984	41,009
March	17,036	21,681
July	7,662	18,113

4.2. Optimal network temperature

The optimized network temperature profile of configuration OPT-DRC is illustrated in Fig. 4. In all months, the network temperature is below the threshold temperature of 14 °C under which direct cooling in data centers is possible. In case of high cooling demands, the network temperature decreases even below the direct cooling threshold temperature of the other buildings (10 °C). In March, the observed temperature fluctuations mainly result from temporal balancing of residual heating and cooling demands using the thermal inertia of the network and ACC. In July, the fluctuations result from the intermittent PV power generation: In times of high PV generation, the temperature of the network and ACC is decreased by an enforced operation of the chiller in the EH. In a subsequent period of low PV generation, the operation of the chiller can be reduced and the temperature of the network and ACC can rise again.

In general, the water mass in the network and the ACC serves different functions in configuration OPT-DRC: During periods with frequently fluctuating heating-to-cooling demand ratios in March, the thermal inertia of the network and ACC is used to balance out residual heating with residual cooling demands over time. In periods with a uniform demand ratio in July,

the network and ACC is predominantly used to increase the onsite utilization rate of PV power. As can be seen from Fig. 4, the thermal inertia of the network and ACC only induce minor fluctuations to an overall constant network temperature level.

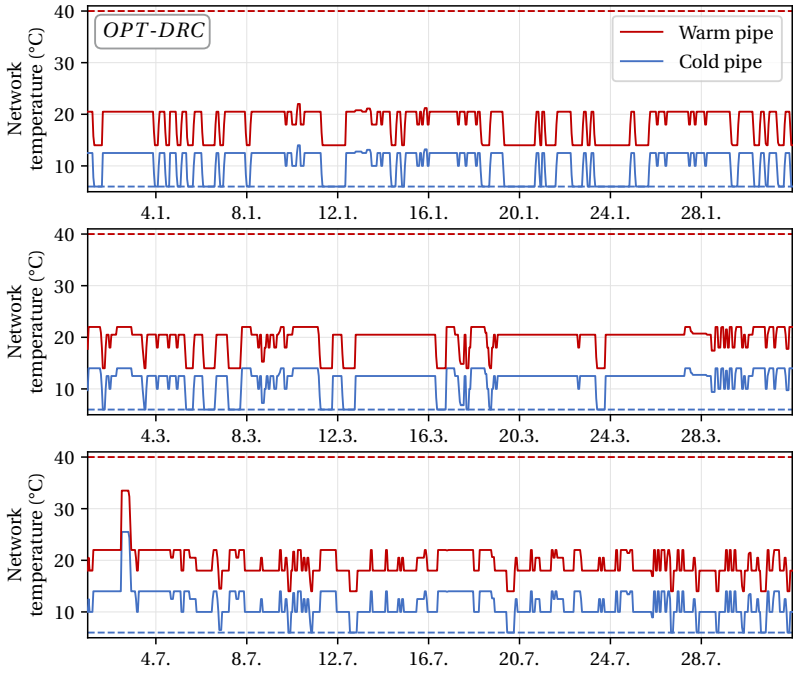

Figure 4: Temperature operation profiles of configuration OPT-DRC (optimized temperature, chillers and direct cooling enabled) for January, March and July.

The network temperatures in scenario OPT are shown in Fig. 5. In January, the mean network temperature remains mostly constant at 27 °C in the warm pipe and 19 °C in the cold pipe. Only three times, the temperature in the warm pipe rises above 30 °C which is caused by a temporary increase of the cooling demand.

In March, the warm pipe temperature fluctuates around 27 °C as well.

However, the fluctuations are larger than in January: Firstly, the COPs of the heat pump and chiller in the EH experience a higher air temperature variation in spring with distinctive day-night cycles. Secondly, the heating-to-cooling demand ratio shows larger fluctuations which cause larger fluctuation of the optimal network temperature.

In July, the optimal temperature in the warm pipe is on average slightly higher (33.5 °C). This is can be explained by the heat dissipation to the ground which reduces the amount of excess heat that has to be removed in the EH. In July, the heat flow to the ground reduces the residual demand by about 5 %. Moreover, the COP of the heat pumps in buildings is increased with high network temperatures. The effect of the network temperature on the performance of the chillers in buildings and in the EH cancel each other out to a large extent: High network temperatures reduce the COP of the building chillers, but at the same time, increase the COP of the chiller in the EH.

The comparison of the configurations OPT-DRC and OPT shows that operating the network at low temperatures and thus enable direct cooling is advantageous, even though this leads to lower COPs of the components in buildings and EH. This effect is quantified and analyzed in more detail in Section 4.3.

4.3. Electricity consumption

In Fig. 6, the electricity balances for both configurations are illustrated. The left bar shows the electricity imported from the grid as well as the PV power generation. On the right, the electricity consumption by electrically-driven system components in the buildings and the EH is displayed. The

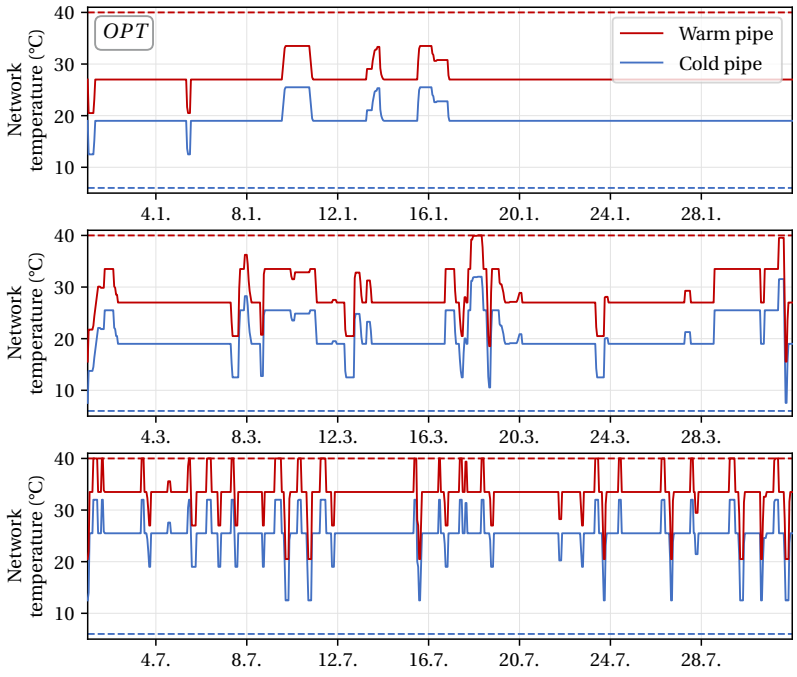

Figure 5: Temperature operation profiles of configuration OPT (optimized temperature, direct cooling disabled) for January, March and July.

electricity demand of all system components is indicated by a dashed line.

The PV generation increases substantially from January to July and accordingly the electricity imported from the power grid decreases. The total electricity demand (dashed line) decreases from January to March but slightly increases from March to July. The reason for low operational costs in March is that large proportions of heating and cooling demands are balanced which substantially reduces the electricity consumption: Although the heating demand decreases from January to March by only 20 % and the cooling demand even rises by 15 %, the electricity consumption of all electrically-driven components decreases by 31 % (OPT-DRC) and 26 % (OPT).

The electricity demand of the system components differs between winter and summer months and strongly depends on the heating-to-cooling demand ratio: In January, the heat generation in buildings (heat pumps and electric boilers) is the largest proportion (80 % in OPT-DRC and 56 % in OPT). A large share of cooling demands are balanced in the system. In scenario OPT, the cold generation by chillers in buildings also takes a substantial proportion (23 %). In July, the electricity demand of chillers dominates and heating demands are mostly balanced in the system: In configuration OPT-DRC, most of the electricity is consumed by the chiller in the EH (67 %). When direct cooling is not enabled (OPT), the electricity demand of chillers in buildings causes 47 % and the central chiller in the EH 43 %. As a result, the total electricity demand of chillers in July with configuration OPT is substantially larger (OPT: 240 MWh, OPT-DRC: 153 MWh).

4.4. Comparison with free-floating temperature operation

In this section, the performance of the optimized temperature operation is compared to the free-floating temperature operation strategy, as described in Section 2.2.8. In Fig. 7, the temperature profile of the free-floating temperature operation is depicted. In January, the network temperatures remain at the lower temperature threshold (6 °C) most of the time since residual heating demands dominate. This shows that direct cooling is also possible with the free-floating temperature operation in months with dominating heating demands. At two occasions (10.01. and 16.01.), residual cooling demands exceed residual heating demands and the temperature of the network reaches the upper temperature limit (40 °C). In March, the network temperatures fluctuate between lower and upper temperature limit due to the frequently

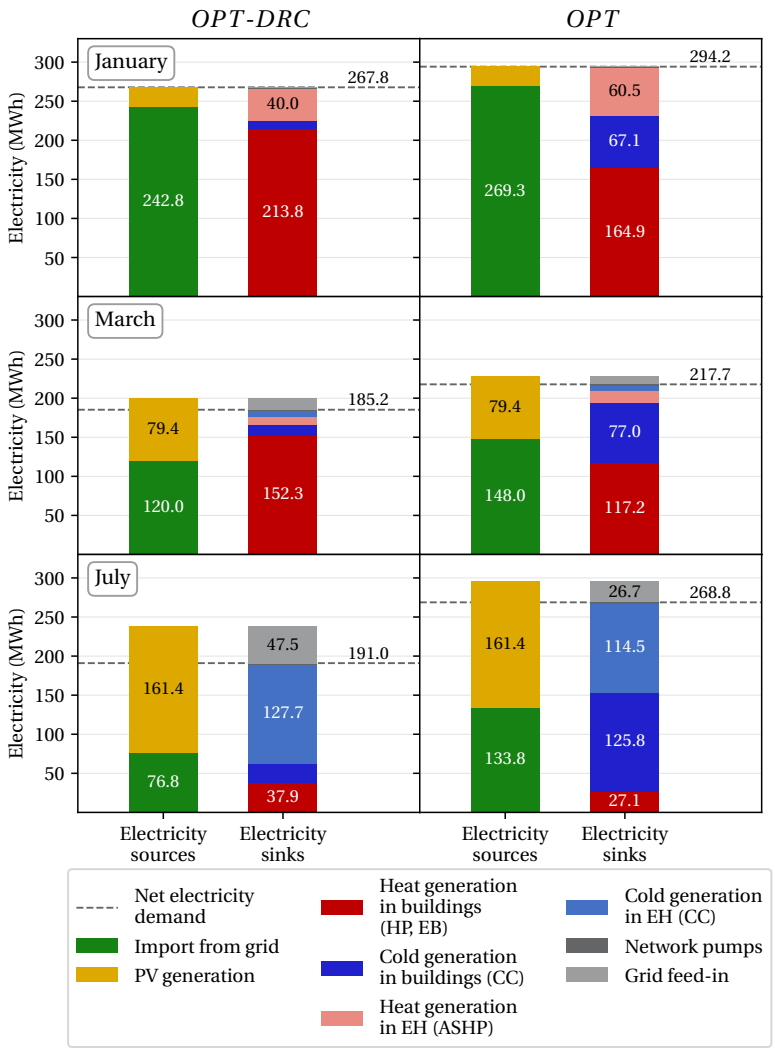

Figure 6: Electricity demand for January, March and July for both configurations OPT-DRC (chillers and direct cooling enabled) and OPT (direct cooling disabled). In all subplots, the bar on the left hand side indicates electricity sources and the bar on the right hand side electricity sinks. The electricity demand of all system components is marked by a dashed line.

alternating residual heating and cooling demands. A constant network temperature is observed in July, since residual cooling dominate throughout the entire month. As a result, direct cooling is not possible during this period.

The optimized temperature operation achieves substantially lower operational costs than the free-floating temperature operation (FF) for two of the three months: In January, the cost savings of the optimized temperature operation (OPT-DRC) are 0.01 % and therefore negligible (operational costs FF: 36,989 EUR). In March, the network temperature optimization results in cost savings of 9.8 % compared to the free-floating approach (FF: 18,897 EUR) and in July 59.7 % (FF: 19,030 EUR). The large cost savings in July result from the high network temperature in the free-floating operation at which direct cooling in buildings cannot be used. As a result, all cooling demands in buildings are covered by chillers which increases the electricity demand and also increases the residual cooling demand to be covered by the EH.

4.5. Comparison with constant network temperatures

In this section, the operational costs of the optimized network temperature profiles are compared with constant network temperatures. For this comparison, 3 temperature pairs for the temperature in the warm and cold pipe are selected: 6 °C/14 °C, 14 °C/22 °C and 22 °C/30 °C. For the comparison, the network temperatures are fixed to the respective values by additional constraints in the optimization model. The optimization is run for the three months January, March and July as well as the two configurations OPT and OPT-DRC. The resulting operational costs are listed in Table 3. For all

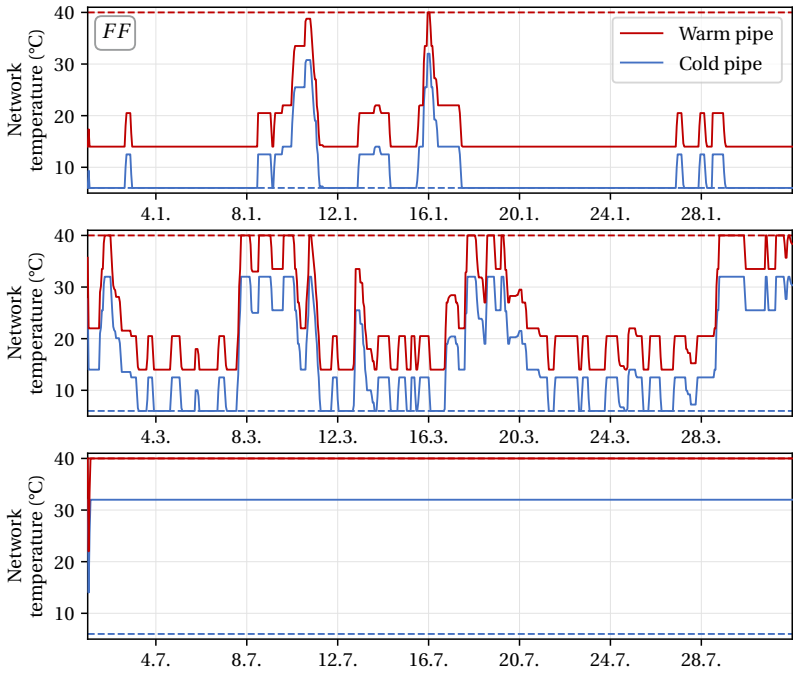

Figure 7: Temperature operation profiles of free-floating temperature operation for January, March and July.

months and configurations, the operational costs are higher with constant temperature profiles than with optimized temperature profiles. This result is expected since the solution space of the optimization is restricted by adding additional constraints to the MILP. The optimization OPT/July with temperatures 6 °C/14 °C does not have a feasible solution (shortage of generation capacity). Across all optimizations, the cost increase ranges between 0.7 % and 143 %. In all months of configuration OPT, the results of the temperature pair 22 °C/30 °C are only slightly higher than the optimized profiles. This indicates that a constant temperature can lead to low operational costs as well. However, this is only the case for certain temperature pairs and

configurations. In general, in at least one season (summer or winter), a fix temperature leads to substantially higher operational costs compared to a flexible temperature optimization.

Table 3: Operational costs (in kEUR) for the constant temperatures profiles and the optimized temperature profiles (corresponding to Table 2).

Configu-ration	Month	Optimized profile (kEUR)	Constant temperature profile (kEUR)					
			6/14 °C		14/22 °C		22/30 °C	
OPT	January	41.0	46.0	+12 %	43.3	+5.6 %	42.0	+2.4 %
OPT	March	21.7	29.8	+37 %	25.3	+17 %	22.4	+3.3 %
OPT	July	18.1	—		21.6	+19 %	18.6	+2.7 %
OPT-DRC	January	37.0	37.2	+0.7 %	37.5	+1.4 %	42.0	+13 %
OPT-DRC	March	17.0	18.4	+7.9 %	17.4	+2.4 %	22.4	+32 %
OPT-DRC	July	7.7	9.0	+17 %	9.0	+17 %	18.6	+143 %

5. Conclusions

In this paper, a mathematical model for the operation optimization of 5GDHC networks is presented. The model proves to be real-time capable and can therefore be used in a model predictive control. The optimization model is applied to a case study with 17 buildings. The cost-optimal network temperature depends on numerous factors with partially opposing influence, of which the following three are the most important:

- The system configuration, i.e. installed technologies in buildings and energy hub, has a strong impact on the optimal network temperature: If heat exchangers for direct cooling are available in buildings, the optimal

network temperature is low enough for the building to be cooled directly with the cold pipe.

- If direct cooling is not possible, the heating-to-cooling demand ratio strongly influences the optimal network temperature.

- Heat losses or gains of the pipe network as well as heat or cold generation efficiencies in the energy hub moderately influence the optimal network temperature.

The thermal inertia of the network and the central thermal storage support the demand balancing and increase the onsite utilization rate of photovoltaics. However, the impact of the network inertia and a medium-sized thermal storage (which balances fluctuations over a day) on the optimal network temperature is small. However, these results cannot be generalized for other system configurations, which use long-term storages with larger volumes or different storage types, like aquifer storages.

The case study shows that direct cooling in buildings is crucial in order to achieve low operational costs. The optimization tends to keep the network temperature below the threshold for direct cooling which results in large cost reductions compared to a free-floating temperature operation, especially in summer months. Even during periods with only small cooling demands, the benefit of direct cooling justifies low network temperatures which result in lower coefficients of performance of heat pumps in buildings. In all scenarios, the optimization model achieves lower operational costs than the operation with constant network temperatures. However, the cost savings strongly depend on the configuration, the selected constant network temperatures

and the season of the year.

In summary, the results show that the developed MILP model is suited for the optimal control of the network temperature of a 5GDHC system. In addition, the model can be used to derive improvements for existing heuristic control approaches, like the free-floating temperature control: If heat exchangers for direct cooling are available in buildings, the operation strategy should give high priority on limiting the network temperature during times with cooling demands. If direct cooling is not possible in buildings, high network temperatures during summer are beneficial since excess heat is dissipated to the ground.

6. Acknowledgments

We gratefully acknowledge the financial support by Federal Ministry for Economic Affairs and Energy (BMWi), promotional reference 03EWR020E (*Reallabor der Energiewende: TransUrban.NRW*).

7. Nomenclature

Abbreviations

5GDHC	5th Generation District Heating and Cooling
ACC	Accumulator Tank
ASHP	Air source heat pump
BES	Building Energy System
CC	Compression Chiller
COP	Coefficient of Performance
DOC	Demand Overlap Coefficient
DRC	Direct Cooling
EB	Electric Boiler
EH	Energy Hub
FF	Free-floating temperature control
HP	Heat Pump
MILP	Mixed-Integer Linear Program
MINLP	Mixed-Integer Nonlinear Program
OPT	Optimized temperature control (no DRC)
OPT-DRC	Optimized temperature control (with DRC)
PV	Photovoltaics
TES	Thermal Energy Storage

Indices and Sets

$b \in \mathrm{B}$	buildings
$t \in \mathcal{T}$	time steps
k	set of temperature intervals

Variables

ΔT Temperature difference

Θ Binary variable (temperature interval)

C Total costs

P Electric power

Q Thermal energy

$\dot{Q}$ Thermal power

S Storage level

T Temperature

$\overline{T}$ Mean temperature

y Binary variable (operation on/off)

Parameters

Δt Duration of time step

η Efficiency

ρ Density

c Specific heat capacity

kA Heat loss coefficient

m Mass

M Big-M

p Price

R Demand ratio

V Volume

Subscripts and Superscripts

c	cooling
cap	capacity
cp	cold pipe
dec	decrease
dem	demand
el	electric
feed-in	feed-in
grid	grid
h	heating
inc	increase
int	interval
loss	network loss
low	lower
max	maximum
min	minimum
netw	network
nom	nominal capacity
op	operational
res	residual
soil	soil
sup	supply
tot	total
up	upper
w	warm
W	water
wp	warm pipe

Appendix A. Demand metrics

The heating-to-cooling demand ratio R indicates whether heating demands $\mathrm{Q}^{\mathrm{tot}}_{\mathrm{h,dem}}$ or cooling demands $\mathrm{Q}^{\mathrm{tot}}_{\mathrm{c,dem}}$ dominate [39]:

$$\mathrm{R} = \frac{\mathrm{Q}^{\mathrm{tot}}_{\mathrm{h,dem}} - \mathrm{Q}^{\mathrm{tot}}_{\mathrm{c,dem}}}{\mathrm{Q}^{\mathrm{tot}}_{\mathrm{h,dem}} + \mathrm{Q}^{\mathrm{tot}}_{\mathrm{c,dem}}} \tag{A.1}$$

R becomes -1 if there is only cooling demand and $+1$ if there is only heating demand. For $R = 0$ the total heating demand equals the total cooling demand.

The demand overlap coefficient DOC describes the overlap of heating and cooling demand profiles, and thus the theoretical demand balancing potential in 5GDHC networks [39]. The DOC ranges between 0 (no overlap) and 1 (heating and cooling demand profiles identical) and is defined as

$$DOC = \frac{2 \cdot \sum_{t \in \mathcal{T}} \min \left\{ \dot{Q}_{\mathrm{h,dem},t}, \dot{Q}_{\mathrm{c,dem},t} \right\}}{\sum_{t \in \mathcal{T}} \left(\dot{Q}_{\mathrm{h,dem},t} + \dot{Q}_{\mathrm{c,dem},t} \right)} \tag{A.2}$$

with $\dot{Q}_{\mathrm{h,dem},t}/\dot{Q}_{\mathrm{c,dem},t}$ as the heating/cooling demand at time step t.

Appendix B. Additional model constraints

All model constraints not mentioned in the main text are listed in the following. These constraints are adapted from the formulation presented in [32].

Appendix B.1. Building energy system

The heating demand $\dot{Q}_{\mathrm{h,dem},b,t}$ equals the heat generation of the heat pump, electric boiler and the net thermal power of the heat storage:

$$\begin{aligned}&\dot{Q}_{\mathrm{h,HP},b,t} + \dot{Q}_{\mathrm{h,EB},b,t} + \dot{Q}^{\mathrm{dch}}_{\mathrm{h,TES},b,t} = \\ &\dot{Q}_{\mathrm{h,dem},b,t} + \dot{Q}^{\mathrm{ch}}_{\mathrm{h,TES},b,t} \quad \forall\, t \in \mathcal{T},\ b \in \mathrm{B}\end{aligned} \tag{B.1}$$

Similarly, the cold generation of the compression chiller and direct cooling equals the cooling demand:

$$\dot{Q}_{\mathrm{c,CC},b,t} + \dot{Q}_{\mathrm{c,DRC},b,t} = \dot{Q}_{\mathrm{c,dem},b,t} \quad \forall\, t \in \mathcal{T},\ b \in \mathrm{B} \tag{B.2}$$

The thermal output of electric boilers is linked with the electricity consumption by a constant thermal efficiency:

$$\dot{Q}_{\mathrm{h,EB},b,t} = P_{\mathrm{EB},b,t}\ \eta_{\mathrm{EB}} \quad \forall\, t \in \mathcal{T},\ b \in \mathrm{B} \tag{B.3}$$

The thermal output of each unit is limited by its rated power:

$$\dot{Q}_{\mathrm{h},k,b,t} \leq \dot{\mathrm{Q}}^{\mathrm{nom}}_{\mathrm{h},u,b} \quad \forall\, u \in \{\mathrm{HP}, \mathrm{EB}\},\ \ t \in \mathcal{T},\ b \in \mathrm{B} \tag{B.4}$$

$$\dot{Q}_{\mathrm{c},k,b,t} \leq \dot{\mathrm{Q}}^{\mathrm{nom}}_{\mathrm{c},u,b} \quad \forall\, u \in \{\mathrm{CC}, \mathrm{DRC}\},\ \ t \in \mathcal{T},\ b \in \mathrm{B} \tag{B.5}$$

The state of charge of the thermal energy storage $S_{\mathrm{TES},b,t}$ is limited by the nominal storage capacity:

$$S_{\mathrm{TES},b,t} \leq \mathrm{S}^{\mathrm{cap}}_{\mathrm{TES},b} \quad \forall\, t \in \mathcal{T},\ b \in \mathrm{B} \tag{B.6}$$

The state of charge of the building heat storage is connected with the state

of charge of the previous time step by

$$S_{\mathrm{TES},b,t} = S_{\mathrm{TES},b,t-1}(1 - \phi_{\mathrm{TES,loss}}) + \eta^{\mathrm{ch}}_{\mathrm{TES}} \dot{Q}^{\mathrm{ch}}_{\mathrm{h,TES},b,t} - \frac{\dot{Q}^{\mathrm{dch}}_{\mathrm{h,TES},b,t}}{\eta^{\mathrm{dch}}_{\mathrm{TES}}} \quad \forall\, t \in \mathcal{T} :\ t \neq t_0,\ b \in \mathrm{B} \tag{B.7}$$

Appendix B.2. Energy hub

The thermal output of the air source heat pump and chiller in the EH is limited by the rated power:

$$\dot{Q}_{\mathrm{h,ASHP},t} \leq \dot{\mathrm{Q}}^{\mathrm{nom}}_{\mathrm{h,ASHP}} \quad \forall\, t \in \mathcal{T} \tag{B.8}$$

$$\dot{Q}_{\mathrm{c,CC},t} \leq \dot{\mathrm{Q}}^{\mathrm{nom}}_{\mathrm{c,CC}} \quad \forall\, t \in \mathcal{T} \tag{B.9}$$

PV power is the product of the global tilted irradiance, module area and electric efficiency:

$$P_{\mathrm{PV}} = \mathrm{G_{sol}}\, \mathrm{A_{PV}}\, \eta_{\mathrm{PV},t} \quad \forall\, t \in \mathcal{T} \tag{B.10}$$

The state of charge of the ACC is limited by the storage capacity:

$$S_{\mathrm{ACC},t} \leq \mathrm{S}^{\mathrm{cap}}_{\mathrm{ACC}} \quad \forall\, t \in \mathcal{T} \tag{B.11}$$

References

[1] European Comission, An EU strategy on heating and cooling, COM(2016) 51 final (2016).

[2] U. Persson, M. Münster, Current and future prospects for heat recovery from waste in european district heating systems: A literature and data review, Energy 110 (2016) 116–128 (2016). doi:10.1016/j.energy.2015.12.074.

[3] S. Boesten, W. Ivens, S. C. Dekker, H. Eijdems, 5th generation district heating and cooling systems as a solution for renewable urban thermal energy supply, Advances in Geosciences 49 (2019) 129–136 (2019). doi:10.5194/adgeo-49-129-2019.

[4] P. Huang, B. Copertaro, X. Zhang, J. Shen, I. Löfgren, M. Rönnelid, J. Fahlen, D. Andersson, M. Svanfeldt, A review of data centers as prosumers in district energy systems: Renewable energy integration and waste heat reuse for district heating, Applied Energy 258 (2020) 114109 (2020). doi:10.1016/j.apenergy.2019.114109.

[5] I. Franzén, L. Nedar, M. Andersson, Environmental comparison of energy solutions for heating and cooling, Sustainability 11 (24) (2019) 7051 (2019). doi:10.3390/su11247051.

[6] The European Comission, Fifth generation, low temperature, high exergy district heating and cooling networks (2015).
URL `https://cordis.europa.eu/project/rcn/194622/factsheet/en`

[7] B. Sanner, R. Kalf, A. Land, K. Mutka, P. Papillon, G. Stryi-Hipp, W. Weiss, 2020-2030-2050, Common vision for the renewable heating and cooling sector in Europe: European technology platform on renewable heating and cooling, Publications Office, Luxembourg, 2011 (2011).

[8] S. Buffa, M. Cozzini, M. D'Antoni, M. Baratieri, R. Fedrizzi, 5th generation district heating and cooling systems: A review of existing cases in europe, Renewable and Sustainable Energy Reviews 104 (2019) 504–522 (2019). doi:10.1016/j.rser.2018.12.059.

[9] J. von Rhein, G. P. Henze, N. Long, Y. Fu, Development of a topology analysis tool for fifth-generation district heating and cooling networks, Energy Conversion and Management 196 (2019) 705–716 (2019). doi:10.1016/j.enconman.2019.05.066.

[10] R. Rogers, V. Lakhian, M. Lightstone, J. S. Cotton, Modeling of low temperature thermal networks using historical building data from district energy systems, in: Proceedings of the 13th International Modelica Conference, Regensburg, Germany, March 4–6, 2019, Linköping Electronic Conference Proceedings, Linköping University Electronic Press, 2019, pp. 543–550 (2019). doi:10.3384/ecp19157543.

[11] F. Bünning, M. Wetter, M. Fuchs, D. Müller, Bidirectional low temperature district energy systems with agent-based control: Performance comparison and operation optimization, Applied Energy 209 (2018) 502–515 (2018). doi:10.1016/j.apenergy.2017.10.072.

[12] A. Prasanna, V. Dorer, N. Vetterli, Optimisation of a district energy system with a low temperature network, Energy 137 (2017) 632–648 (2017). doi:10.1016/j.energy.2017.03.137.

[13] M. Pellegrini, A. Bianchini, The innovative concept of cold district heating networks: A literature review, Energies 11 (1) (2018) 236 (2018). doi:10.3390/en11010236.

[14] F. Ruesch, M. Haller, Potential and limitations of using low-temperature district heating and cooling networks for direct cool-

ing of buildings, Energy Procedia 122 (2017) 1099–1104 (2017). doi:10.1016/j.egypro.2017.07.443.

[15] T. Sommer, S. Mennel, M. Sulzer, Lowering the pressure in district heating and cooling networks by alternating the connection of the expansion vessel, Energy 172 (2019) 991–996 (2019). doi:10.1016/j.energy.2019.02.010.

[16] W. H. Song, Y. Wang, A. Gillich, A. Ford, M. Hewitt, Modelling development and analysis on the balanced energy networks (ben) in London, Applied Energy 233-234 (2019) 114–125 (2019). doi:10.1016/j.apenergy.2018.10.054.

[17] A. Revesz, P. Jones, C. Dunham, G. Davies, C. Marques, R. Matabuena, J. Scott, G. Maidment, Developing novel 5th generation district energy networks, Energy 201 (2020) 117389 (2020). doi:10.1016/j.energy.2020.117389.

[18] F. Ruesch, R. Evins, District heating and cooling with low temperature networks – sketch of an optimization problem: Coleb workshop, 6.-7. march 2014. eth zürich. (2014).

[19] A. Prasanna, V. Dorer, N. Vetterli, Optimisation of a district energy system with a low temperature network, Energy 137 (2017) 632–648 (2017). doi:10.1016/j.energy.2017.03.137.

[20] S. Buffa, A. Soppelsa, M. Pipiciello, G. Henze, R. Fedrizzi, Fifth-Generation District Heating and Cooling Substations: Demand Re-

sponse with Artificial Neural Network-Based Model Predictive Control, Energies 13 (17) (2020) 4339 (2020). doi:10.3390/en13174339.

[21] M. Mohanraj, S. Jayaraj, C. Muraleedharan, Applications of artificial neural networks for refrigeration, air-conditioning and heat pump systemsA review, Renewable and Sustainable Energy Reviews 16 (2011) 1340–1358 (2011). doi:10.1016/j.rser.2011.10.015.

[22] P. Gabrielli, A. Acquilino, S. Siri, S. Bracco, G. Sansavini, M. Mazzotti, Optimization of low-carbon multi-energy systems with seasonal geothermal energy storage: The Anergy Grid of ETH Zurich, Energy Conversion and Management: X (2020) 100052 (2020).

[23] T. Blacha, M. Mans, P. Remmen, D. Müller, Dynamic simulation of bidirectional low-temperature networks – A case study to facilitate the integration of renewable energies, Building Simulation Conference (2019).

[24] R. Zarin Pass, M. Wetter, M. A. Piette, A thermodynamic analysis of a novel bidirectional district heating and cooling network, Energy 144 (2018) 20–30 (2018). doi:10.1016/j.energy.2017.11.122.

[25] A. Vandermeulen, B. van der Heijde, L. Helsen, Controlling district heating and cooling networks to unlock flexibility: A review, Energy 151 (2018) 103–115 (2018). doi:10.1016/j.energy.2018.03.034.

[26] B. Bøhm, Simple models for operational optimisation, Vol. 2002,S1 of IEA district heating, Netherlands Agency for Energy and the Environment, 2002 (2002).

[27] A. Benonysson, B. Bøhm, H. F. Ravn, Operational optimization in a district heating system, Energy Conversion and Management 1995 (36) (1995) 297–314 (1995).

[28] M. Leśko, W. Bujalski, Modeling of district heating networks for the purpose of operational optimization with thermal energy storage, Archives of Thermodynamics 38 (4) (2017) 139–163 (2017). doi:10.1515/aoter-2017-0029.

[29] S. Grosswindhager, A. Voigt, M. Kozek, Predictive control of district heating network using fuzzy dmc, in: 2012 Proceedings of International Conference on Modelling, Identification and Control, 2012, pp. 241–246 (2012).

[30] L. Merkert, A. Haime, S. Hohmann, Optimal scheduling of combined heat and power generation units using the thermal inertia of the connected district heating grid as energy storage, Energies 12 (2) (2019) 266 (2019). doi:10.3390/en12020266.

[31] W. Gu, J. Wang, S. Lu, Z. Luo, C. Wu, Optimal operation for integrated energy system considering thermal inertia of district heating network and buildings, Applied Energy 199 (2017) 234–246 (2017). doi:10.1016/j.apenergy.2017.05.004.

[32] M. Wirtz, L. Kivilip, P. Remmen, D. Müller, 5th generation district heating: A novel design approach based on mathematical optimization, Applied Energy 260 (2020) 114158 (2020). doi:10.1016/j.apenergy.2019.114158.

[33] J. Kallrath, Gemischt-ganzzahlige Optimierung: Modellierung in der Praxis, Springer Fachmedien Wiesbaden, Wiesbaden, 2013 (2013). doi:10.1007/978-3-658-00690-7.

[34] R. G. Jeroslow, J. K. Lowe, Modelling with integer variables, in: R. W. Cottle, L. C. W. Dixon, B. Korte, M. J. Todd, E. L. Allgower, W. H. Cunningham, J. E. Dennis, B. C. Eaves, R. Fletcher, D. Goldfarb, J.-B. Hiriart-Urruty, M. Iri, R. G. Jeroslow, D. S. Johnson, C. Lemarechal, L. Lovasz, L. McLinden, M. J. D. Powell, W. R. Pulleyblank, A. H. G. Rinnooy Kan, K. Ritter, R. W. H. Sargent, D. F. Shanno, L. E. Trotter, H. Tuy, R. J. B. Wets, E. M. L. Beale, G. B. Dantzig, L. V. Kantorovich, T. C. Koopmans, A. W. Tucker, P. Wolfe, B. Korte, K. Ritter (Eds.), Mathematical Programming at Oberwolfach II, Vol. 22 of Mathematical Programming Studies, Springer Berlin Heidelberg, Berlin, Heidelberg, 1984, pp. 167–184 (1984). doi:10.1007/BFb0121015.

[35] J. K. Jensen, T. S. Ommen, L. Reinholdt, W. B. Markussen, B. Elmegaard, Heat pump COP, part 2: Generalized COP estimation of heat pump processes, Proceedings of the13th IIR-Gustav Lorentzen Conference on Natural Refrigerants (2018).

[36] J. Bisschop, AIMMS Optimization Modeling (2018).

[37] BDEW-Strompreisanalyse Januar 2020.

[38] Bundesnetzagentur, Archivierte EEG-Vergütungssätze und Datenmeldungen.

[39] M. Wirtz, L. Kivilip, P. Remmen, D. Müller, Quantifying Demand Balancing in Bidirectional Low Temperature Networks, Energy and Buildings 224 (2020) 110245 (2020). doi:10.1016/j.enbuild.2020.110245.

[40] K.-K. Cao, K. von Krbek, M. Wetzel, F. Cebulla, S. Schreck, Classification and Evaluation of Concepts for Improving the Performance of Applied Energy System Optimization Models, Energies 12 (24) (2019) 4656 (2019). doi:10.3390/en12244656.